# LATERAL-LOAD RESPONSE OF TWO REINFORCED CONCRETE BENTS

By Marc O. Eberhard[1] and M. Lee Marsh,[2] Associate Members, ASCE

**ABSTRACT:** Two reinforced concrete bridge bents were subjected to large, transverse displacements. The bents contained detailing deficiencies typical of the 1960s, including minimal transverse reinforcement, short reinforcing splices, and a lack of top reinforcement in the footings. Spalling of the concrete cover at the column tops began at a drift ratio of 1.5%. At this drift ratio, the column displacement ductility was approximately four, the curvature ductility was eight, and nominal curvature in the plastic hinges corresponded to a nominal maximum concrete strain of 0.01. In spite of their deficiencies, the bents resisted transverse loads equal to nearly 40% of the bridge's weight at a drift ratio of 3%. The ductile response was attributed to a low shear demand and to the influence of the soil in redistributing the rotational demands away from the column splices. The measured response was reproduced well by an analytical model that considered the nonlinear force-deformation relationships of the columns and soil. The results of a parametric study indicated that the soil surrounding the column bases increased the column shear demand by 25%.

## INTRODUCTION

Extensive testing has been directed at predicting the resistance of reinforced concrete components to cyclic displacements. On the basis of such tests and of experience gained during past earthquakes, many investigators have identified deficiencies in existing components and have developed retrofit schemes that increase the earthquake resistance of older reinforced concrete bridges (e.g., Priestley et al. 1992; Thewalt and Stojadinovic 1995). In contrast, few destructive, lateral-load tests of structural systems have been performed, and little data is available to calibrate analytical models of the large-displacement seismic response of bridges.

The planned demolition of a pair of obsolete reinforced concrete bridges provided the opportunity to measure the transverse force-displacement response of one of these three-span bridges (Fig. 1) (Eberhard et al. 1993). Eberhard and Marsh (1997) discuss tests and analyses of the bridge in its initial state, in which two bents and two abutments provided the bridge's resistance to transverse loads. Although the bridge was constructed in 1966 and was not designed to resist significant lateral loads, the bridge was extremely stiff and strong. The bridge resisted a transverse load (3,400 kN) equal to 65% of the bridge's weight at a bent displacement (12 mm) equal to 0.2% of the clear column height. The bridge's large initial strength and stiffness were attributed to the bridge's continuous superstructure and the resistance that the abutments provided.

This paper analyzes a second series of tests, in which the bents [Fig. 1(b)] were subjected to drift ratios of up to 3%. The objectives of the bent tests and analyses were as follows:

1. To measure the stiffness, strength, and toughness of the bents
2. To estimate the vulnerability of similar bents
3. To compare the observed response with that computed with an analytical model
4. To investigate the sensitivity of the computed response to several modeling options

O'Donovan et al. (1994) provide details of the tests.

## DESCRIPTION OF BENTS

The bents that were tested served as the intermediate supports for the bridge shown in Fig. 1. This three-span bridge had been constructed in 1966 to carry two lanes of east-bound traffic (Interstate-90) over a railroad line. The two exterior spans measured 12.5 m each, and the center span measured 18.3 m [Fig. 1(a)]. The superstructure consisted of a 165-mm thick reinforced concrete slab that was supported by six prestressed concrete I-girders [Fig. 1(b)]. The abutments consisted of a diaphragm and two wingwalls that rested on a pedestal [Fig. 1(c)]. Eberhard and Marsh (1997) provide details of the superstructure and abutments.

Fig. 2 shows an elevation of the bents. To make the structure continuous for resisting live loads, the bridge designers had provided a 305-mm thick cast-in-place diaphragm to tie together the slab, I-girders, and the bent crossbeam (Fig. 2, section A-A). The resulting slab/diaphragm/crossbeam combination was more than 2 m thick, and it was much stronger and stiffer than the supporting columns.

The column details were typical of 1960s construction in the United States. The two 915-mm diameter columns were reinforced longitudinally with eleven No. 9 bars (diameter, $d_b$ = 28.6 mm), which corresponds to a longitudinal reinforcement ratio of 1.1%. The column's transverse reinforcement consisted of No. 3 hoops at 305 mm spacings, which provided an equivalent spiral reinforcement ratio of 0.14%. This ratio is less than one tenth of that required by current seismic design codes (*AASHTO* 1994). Although the ends of the hoops overlapped by 350 mm, the hoops' detailing was inadequate because no hooks extended into the column core. The column axial load of 950 kN was relatively low. It corresponded to a compressive stress equal to 5.2% of the specified concrete compressive strength (28 MPa).

The splices were also typical of older reinforced concrete bridges. At the base of the columns, the longitudinal reinforcement was lap spliced to dowels that were embedded in the spread footings. These splices were only 1,000 mm long ($35d_b$), and no additional confinement was provided along the splices' length. In the footings, the dowels were bent to 90° and extended $20d_b$ horizontally away from the columns. The footings were reinforced with No. 8 bars in each direction on the bottom. In contrast to current requirements, the footings had no top reinforcement.

Almost half of each column was embedded in compacted fill. The top-of-footing elevation was 7.6 m below the crossbeam soffit, while the bent was only 12.5 m from the abutment. Consequently, the 2:1 slope intersected the columns at approximately midheight, and the columns were embedded in 3.7 m of fill.

[1]Assoc. Prof., Dept. of Civ. Engrg., Univ. of Washington, Box 352700, Seattle, WA 98195.

[2]Sr. Engr., Berger/Abam Engrs. Inc., Federal Way, WA 98003.

Note. Associate Editor: Chia-Ming Uang. Discussion open until September 1, 1997. To extend the closing date one month, a written request must be filed with the ASCE Manager of Journals. The manuscript for this paper was submitted for review and possible publication on August 1, 1995. This paper is part of the ***Journal of Structural Engineering***, Vol. 123, No. 4, April, 1997. ©ASCE, ISSN 0733-9445/97/0004-0461–0468/$4.00 + $.50 per page. Paper No. 11421.

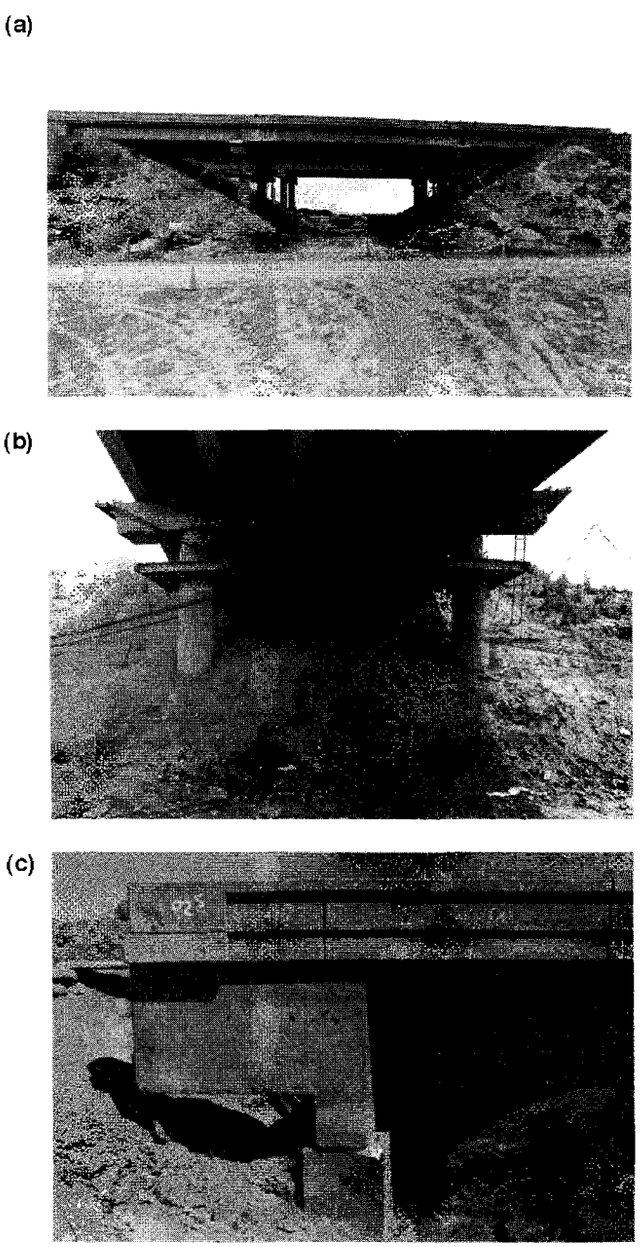


**FIG. 1. Test Bridge: (a) South Elevation; (b) East Bent; (c) Excavated West Abutment**

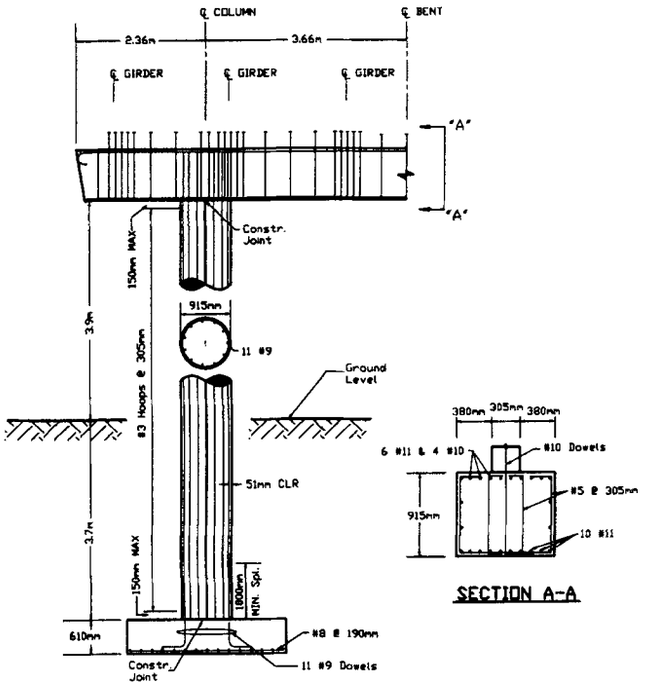


**FIG. 2. Bent Elevation**

**TABLE 1. Material Properties**

| Parameter (1) | Value (2) |
|---|---|
| (*a*) Concrete | |
| Specified minimum compressive strength | 28 MPa |
| Measured compressive strength | 44 MPa |
| (*b*) Steel | |
| Specified minimum yield stress | 275 MPa |
| Measured yield stress | 350 MPa |
| Measured strength | 595 MPa |
| Strain at onset of hardening | 0.008 |
| Strain at peak stress | 0.035 |
| (*c*) Fill | |
| In-situ unit weight | 17.3 kN/m$^3$ |
| Angle of internal friction, $\phi$ | 38° |

The measured material properties for the concrete, reinforcing steel, and fill are reported in Table 1. The concrete strength was measured from 100-mm diameter cores, and the steel properties were measured from two No. 9 steel coupons that were extracted from the columns. The fill's angle of internal friction was measured from undisturbed samples collected at the site and tested under undrained conditions.

## TEST PROGRAM

The goal of the test program was to impose large transverse displacements to the bents and monitor their response. Testing options were constrained by the requirement that the bridge traffic not be disrupted during installation of the loading apparatus and instrumentation.

### Loading

Displacements were imposed on the bents by applying transverse loads to the bent crossbeams. The loads were generated by hydraulic rams, located at ground level, and transmitted to the bents by prestressing strands (Figs. 1 and 3). The applied forces were controlled by varying the pressure in the hydraulic rams, which had been calibrated before the tests. Deadmen on each side of the bridge provided the reactions to the applied loads.

During the tests, cyclic loads were applied to the bents to produce maximum displacements of ±40, 75, 150, and 230 mm in the north-south direction. Two cycles were imposed at each displacement level. Because these displacements corresponded to drift ratios of 0.5, 1, 2, and 3%, the pairs of displacement cycles were designated as tests B5, B1, B2, and B3 (Fig. 4). Typically, a half cycle of loading lasted 2–4 h.

### Superstructure Isolation

To minimize the resistance that the abutments provided, the superstructure was isolated from the abutment pedestal. As shown in Fig. 1(c), the soil that surrounded the abutment diaphragm and wingwalls was excavated. Then, the abutment diaphragm was lifted with hydraulic rams, and the bearing pads and were replaced with isolation devices. The isolation devices consisted of polished, greased stainless-steel plates and ultrahigh-molecular-weight plates (TIVAR-100), all enclosed

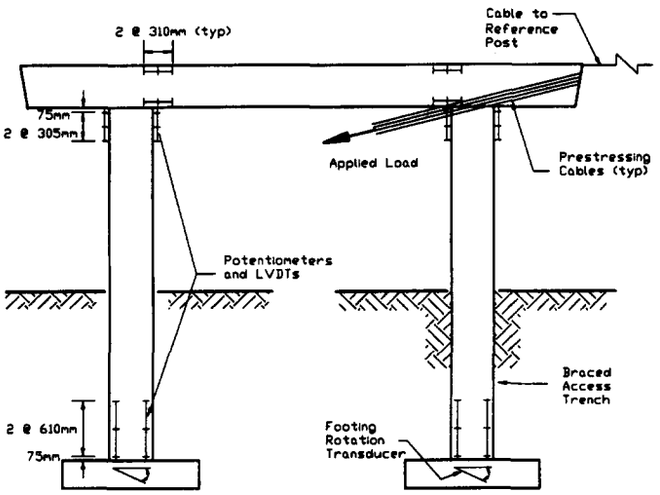


**FIG. 3. West Bent Instrumentation**

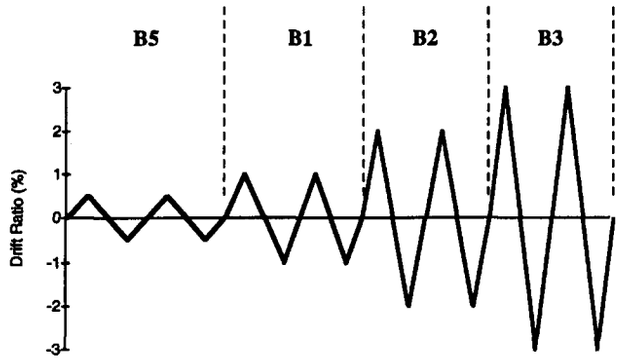


**FIG. 4. Imposed Displacement History**

in polyethylene envelopes. In the laboratory, the coefficient of friction for this combination was measured to be 0.05, but even this small friction decreased under sustained loading. Based on the estimated abutment vertical reaction of 800 kN per abutment, the frictional resistance provided by the isolation system was calculated to be 80 kN. This resistance was approximately equal to 4% of the applied lateral load.

## Instrumentation

The transverse displacements of both bents were measured relative to reference posts located 7 m from the bridge. The instrumentation setup at each bent consisted of a Temposonic transducer that measured the vertical motion of a weight; this weight was connected to the bent by a cable and pulley system. Similar instrumentation monitored the transverse displacements of the abutment diaphragms.

To monitor relative rotations of beam and column cross-sections, threaded rods were epoxied into drilled holes on the column and beam faces (Fig. 3). LVDTs and potentiometers mounted on these rods were used to measure the change in distance between the ends of adjacent rods. Relative rotations were calculated from the relative displacement measurements for pairs of instruments on opposite faces of the column or beam.

On the west bent, 0.75-m wide trenches were excavated on the east side of the columns to provide access to the column bases and to the top of the footings. To minimize the effect of the trenches on the soil resistance, the trenches were oriented perpendicular to the direction of bent motion (the trenches were parallel to the direction of traffic). Clinometers mounted on the footings measured their absolute rotation (Fig. 3).

## OBSERVED RESPONSE

The bent force-displacement history, the observations of recorded damage, and the measured average curvatures provide a summary of the bent's response to the applied loads.

### Bent Force-Displacement Histories

Fig. 5(a) shows the force-displacement history for the bents. The applied forces shown in the figure include the resistance that the isolation system provided (80 kN). This resistance had the effect of increasing the resistance during loading and of decreasing the resistance during unloading. The "notches" in the history near the point of zero load were caused by the viscous nature of the isolation system resistance. At the end of each half-cycle, the bents moved slowly after the applied load was removed as the isolation system resistance dissipated.

The force-displacement relationship was corrected to account for the effect of the isolation system during loading and unloading. The corrected hysteresis curve as shown for a single column is shown in Fig. 5(b). Because the corrections were made assuming that the abutment resistance was perfectly plastic (not viscous), the notches remained in the corrected history. Although the column stiffnesses decreased with increasing drift ratio and repeated cycling, the columns repeatedly provided an average lateral-load resistance of 500 kN. Together, the four columns provided a resistance of 2,000 kN, equal to approximately 3/8 of the bridge's weight (5,300 kN).

### 0.5% Drift Ratio (Test B5)

During the first excursion to a drift ratio of 0.5%, flexural cracks were visible on the tension face of the top 1 m of the

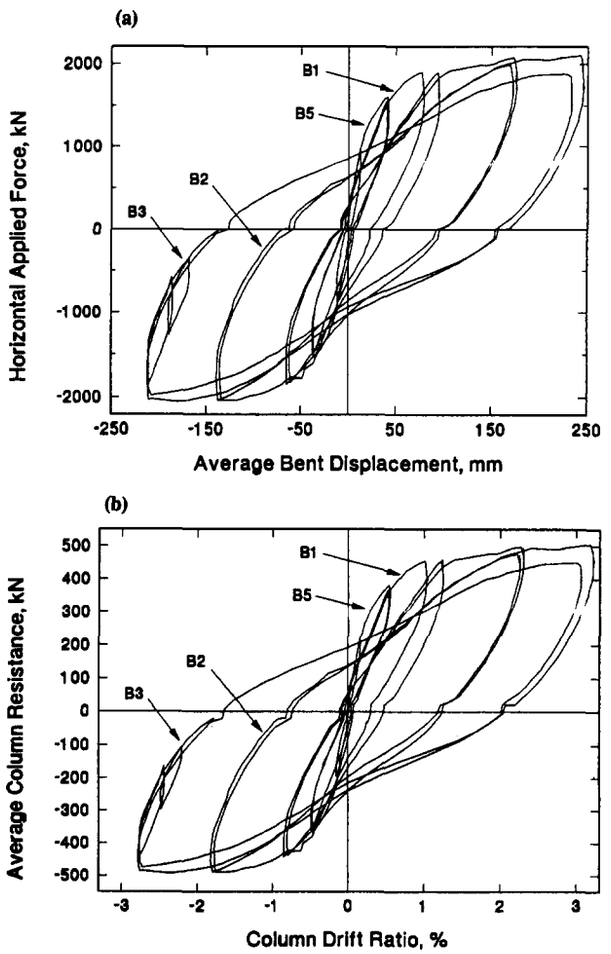


**FIG. 5. Force-Displacement Histories: (a) Applied Horizontal Force; (b) Corrected Column Force**

columns. The maximum crack width at the top of the four columns ranged from 0.5 to 1 mm. At the base of the columns, the cracks were smaller; a few hairline flexural cracks formed at heights ranging from 0.8 to 1.5 m above the footing. After the direction of displacement reversed, the cracks that had opened in the previous half-cycle closed completely. The damage did not increase significantly when the structure was subjected to a second displacement cycle.

### 1% Drift Ratio (Test B1)

Fig. 6(a) shows the extent of damage during the first half cycle to a drift ratio of 1%. In comparison with test B5, the crack sizes increased (maximum width ranged from 2 to 3 mm at the tops of the columns), and new cracks formed on the tension faces. At the bottom of the columns, a few new cracks appeared, the largest being 0.3 mm wide, and the movement of the columns began to induce permanent compressive deformations in the soil surrounding the columns. In the second cycle to the same drift ratio, some cracks did not close completely when the column face went into compression. During the last half cycle, researchers detected a drop of pitch when they tapped the column surface on the tension side of some of the column tops. This drop in pitch was attributed to detachment of the cover from the column cores.

### 2% Drift Ratio (Test B2)

During the first half cycle to a drift ratio of 2%, the maximum crack sizes increased (4–7 mm), and the onset of spalling was apparent on all of the columns. In contrast, the base of the columns had only small cracks. The largest of these cracks, which were only 1–1.5 mm wide, formed in a region that was approximately 1–2 m above the footing. The gap between the column and the surrounding soil increased along the column height. At a height of about 3 m above the footing, the gap between the soil and column was approximately 50 mm. At a height of 0.6 m, the gap closed to approximately 3 mm. Upon repeated loading to a drift ratio of 2%, the tops of all of the columns spalled on both sides.

### 3% Drift Ratio (Test B3)

Fig. 6(b) shows the damage observed during the first excursion to a drift ratio of 3%, the largest drift ratio imposed on the structure. Even during the first half cycle, spalling was widespread in the top 0.6 m of the columns, and diagonal cracks began to form. At the end of the second cycle, the spalling had spread, and buckled bars were visible on all of the columns. Despite the heavy damage to the tops of the columns, no spalling was observed at the base of the columns, no footing damage was observed, and crossbeam damage was limited to minor joint cracking. Fig. 7 shows the damage to the top of northeast column at the end of the tests.

### Column Curvatures

The measured average curvatures (computed as the relative rotations divided by the instrument gauge lengths) were consistent with the observed damage (Fig. 8). Curvatures were largest at the tops of the columns, and the extent of yielding increased with increasing drift ratio. At a drift ratio of 0.5% (test B5), the average curvature exceeded the nominal yield curvature (0.0041/m) over the first instrument gauge length (75 mm). This measurement included any anchorage slip of the reinforcement. The average curvature over the second instrument gauge length (75–380 mm from soffit) exceeded the yield curvature during test B1. The curvature over the third

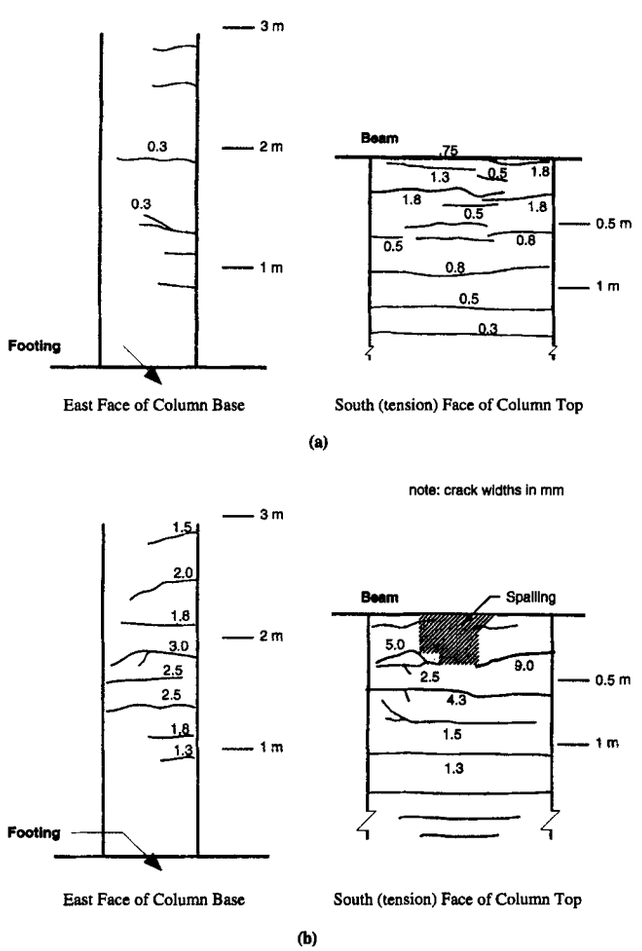


**FIG. 6. Column Damage at Drift Ratios of: (a) 1%; (b) 3%**

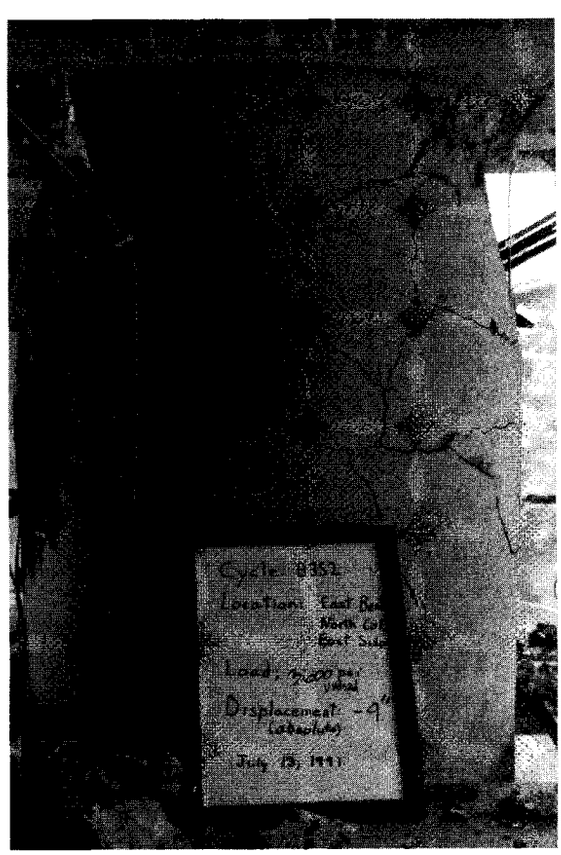

**FIG. 7. Damage at Top of Column at End of Testing**

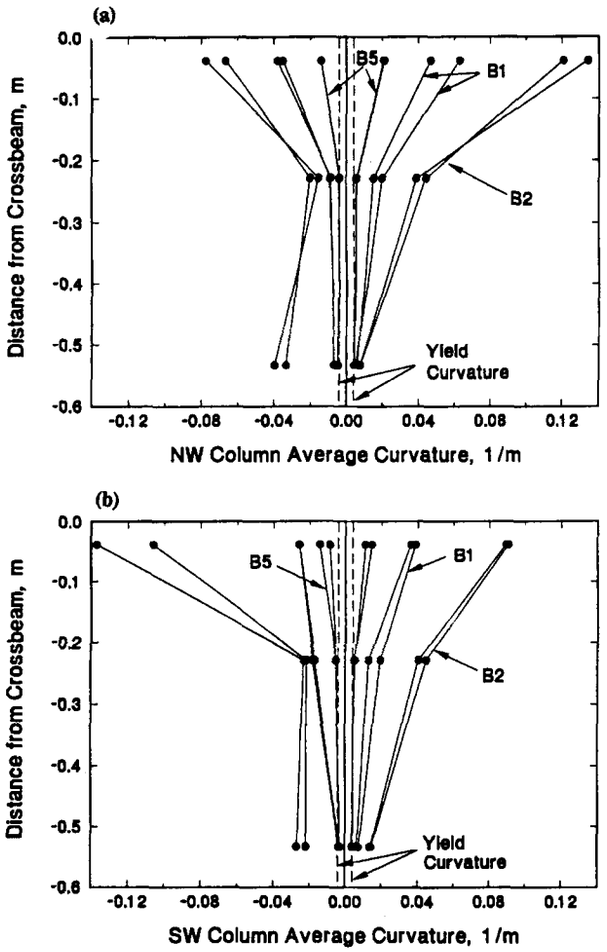


**FIG. 8. Curvature Maxima for West Bent Column Tops**

gauge length (380–685 mm from the soffit) exceeded the yield curvature during test B2. Fig. 8 does not report the curvature distributions for test B3 because extensive spalling and bar buckling interfered with the instruments. In general, the curvatures measured for the second cycle at each drift level were similar to the curvatures measured for the first cycle. Curvature measurements at the column bases were adversely affected by soil and rock that fell into the trenches.

## RELIABILITY OF MEASUREMENTS

Before considering the implications of the measured response, it is important to consider the reliability of the measurements. The measured bent displacements were confirmed intermittently with an electronic distance meter. The applied forces, which were calculated from measured hydraulic ram pressures, were verified by comparing them with the elongation of one of the prestressing strands over a 610 mm length (O'Donovan et al. 1994).

The deck deformation history, which was computed as the average bent displacement minus the average abutment displacement, suggested that the isolation system was effective in minimizing the abutment resistance. For example, despite the fact that the bent displacements were approximately ±75 mm for test B1, the deck deformation varied by only ±0.6 mm.

The relative rotation measurements were similar at the top of all four columns (coefficient of variation = 5%). The rotations were also consistent with the measured drift ratios (Fig. 9). The magnitude of the rotation measured in the first 0.7 m of the four columns was equal to 70% of the measured drift ratio for test B5, the rotation was equal to 85% of the drift

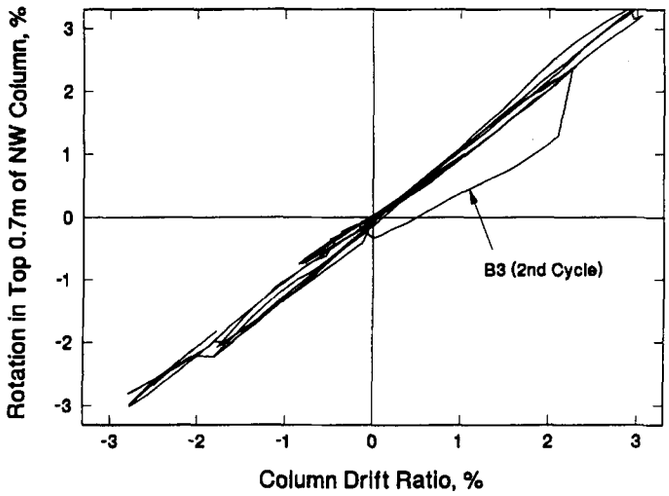


**FIG. 9. Consistency of Rotation and Displacement Measurements**

ratio for test B1, and the rotation was equal to 110% of the average rotation for test B2. This increase in the fraction of deformation concentrated at the top of the column was consistent with formation of a hinge at the column top.

## IMPLICATIONS OF OBSERVED RESPONSE

The tests' results also provided the opportunity to compare the measured response with design recommendations and to estimate the seismic vulnerability of the bents.

### Plastic Hinge Rotations

As part of the evaluation of a bridge's seismic vulnerability, it is common to estimate the displacement ductility capacity, $\mu$, with plastic hinge analysis (Park and Paulay 1975). To calibrate such evaluation procedures, it is useful to relate the observed damage to the computed member displacement ductility, the curvature ductility, and the nominal concrete compressive strain. The comparison will be made at a drift ratio of 1.5%, the point at which significant spalling began.

The member displacement ductility for the column top cannot be derived directly from Fig. 5(b) because the boundary conditions at the tops and bottoms of the columns were not the same. An approximate estimate of the member displacement ductility was computed based on two assumptions: (1) the distance, $\ell$, from the soffit to the inflection point was 3.2 m; and (2) half of the total deflection occurred above the inflection point. The two assumptions were equivalent to assuming that the column was fixed at an elevation above the footing equal to 1/3 of the fill depth. Combining the calculated yield curvature ($\phi_y$ = 0.0041/m) and the approximate value for $\ell$, the yield displacement was estimated at 28 mm. The corresponding drift ratio of 0.4% is reasonable when compared with Fig. 5(b). Therefore, the top-of-column displacement ductility ratio, $\mu$, at the onset of spalling at the column top (drift ratio = 1.5%) was approximately equal to 4.

To estimate the curvature ductility, it was necessary to assume a plastic hinge length. Paulay and Priestley (1992) proposed that the plastic hinge length, $\ell_p$, be computed as follows:

$$\ell_p = 0.08\ell + 0.022 d_b f_y \text{ (MPa)} \quad (1)$$

where $d_b$ = bar diameter (28.6 mm); and $f_y$ = yield stress (350 MPa). The resulting plastic hinge length of 450 mm was approximately equal to half of the column diameter (915 mm). Combining $\mu$ = 4 and $\ell_p/\ell$ = 0.14, the curvature ductility ratio

was found to be 9 at the onset of spalling (Park and Paulay 1975). At the corresponding curvature (0.036/m), the moment-curvature analysis indicated that the nominal maximum concrete compressive strain was 0.01.

### Shear Capacity

Although shear cracks formed in the last two cycles (B3), the tests did not measure the shear capacity of the columns because they did not fail in shear. Nonetheless, the column resistance measured during the test (Fig. 5) provided a lower bound on the columns' shear strength at large displacements. At the end of the test, the drift ratio was 3%, the member displacement ductility demand was 8, and the curvature ductility demand was 18.

The observed lower bound on shear strength can be compared with design recommendations by Priestley et al. (1994). According to their procedure, the shear resistance, $V_p$, attributable to the axial force is $V_p = P \tan \alpha$, where $P$ is the axial load and $\alpha$ is the angle of inclination of the axial load. Considering the overturning moment and the vertical component of the applied bent load (Fig. 3), the axial load carried by the compression-side column was estimated as 1,250 kN. The value of tan $\alpha$ was computed as 0.11 based on the effective column length of 2 × 3.2 m and an effective depth of 0.8 × 905 mm. Combining these values, $V_p$ was estimated as 140 kN. The shear force attributable to the steel was calculated as 180 kN, and the concrete component of shear resistance was estimated as 350 kN for large displacement ductilities ($\mu > 4$). Therefore, the total available shear capacity was estimated as 670 kN for the compression side column.

In comparison, the average column shear was measured to be 500 kN [Fig. 5(b)]. Taking into account the increase in flexural capacity in the compression-side column due to the increased axial load, the compression column likely resisted a shear of approximately 550 kN. Therefore, it appears that the observed response was consistent with the Priestley et al. (1994) design recommendations. Furthermore, assuming the axial and steel components of resistances are correct, the concrete must be assigned a resistance of at least 230 kN to rationalize the observed shear capacity. If the steel contribution is neglected because some of the hoops unwrapped at large drifts, the concrete must be assigned a resistance of at least 410 kN. In either case, unless the shear resistance of the axial load and steel components are significantly increased, a substantial component of shear resistance must be attributed to the concrete to explain the observed shear strengths at large displacements.

### Seismic Vulnerability

The vulnerability of the bents to transverse motions can be estimated from the measured test response. To make this estimate, the isolated bridge was modeled as a single-degree-of-freedom, elastoplastic system with a yield force (2,000 kN) equal to 3/8 of its weight and a yield displacement equal to 50 mm (Fig. 5). The initial period for such a system is 0.73 s. It was assumed that the displacements of the nonlinear system could be estimated with linear response spectrum analysis. In general, the response spectrum varies with the site conditions, but for simplicity, the ground motion was assumed to have a dynamic amplification factor of 2.5. This factor is consistent with the maximum amplification coefficient required by current bridge codes (*AASHTO* 1994).

A ground motion with an effective peak acceleration of $0.2g$ would produce a displacement of approximately 2.5 × 0.2 × 50/(3/8) = 67 mm, which corresponds to a drift ratio of roughly 0.9%. At this drift ratio, the damage observed in the tests was limited to minor flaking of the concrete and flexural cracks. At an effective acceleration of $0.4g$, the estimated displacement increases to 133 mm (drift ratio 1.8%), and spalling would be expected. At an effective acceleration of $0.6g$, the calculated displacement is 200 mm (drift ratio of 2.6%). The tests demonstrated that major spalling would be expected at this displacement but that the bents would be unlikely to collapse. Of course, the effects of biaxial loading, vertical motions, and strain rate would modify the behavior during an actual earthquake.

### Extrapolation to Other Bridges

The extent to which the response of the tested bents can be extrapolated to other bridges depends on the extent to which the bents are similar. Many bridges have similar deficiencies because it was standard practice before 1971 to provide little transverse reinforcement, to place short lap splices at the footing construction joint, and to omit top footing reinforcement. The test results are particularly relevant to bridges in which the abutment resistance has little influence on the bent displacements. Such bridges include long bridges, bridges with expansion joints at intermediate bents, and bridges without shear keys at the abutments.

The test bridge columns had a column reinforcement ratio of 1.1% and a compressive axial stress equal to 3.3% of the actual concrete compressive strength (Table 1). Other bridge bents would be more brittle if their columns have more flexural reinforcement or a higher axial load than the test bridge columns. The effect of the soil would be smaller in bents with less fill surrounding the columns. If the soil embedment had been smaller, the bents would have been more flexible, they would have had lower shear demands, and the splices would likely have been damaged. The cast-in-place bent diaphragms also affected the vulnerability. Because the crossbeams were much stronger and stiffer than the columns, the crossbeams were not damaged, and damage was concentrated at the tops of the columns. If the crossbeams had been weaker and more flexible, it is likely that the crossbeam would have been damaged more and that the top of the columns would have been damaged less at a given drift ratio.

## ANALYTICAL MODEL

For seismic assessments, it is becoming increasingly common to model bridges embedded in soil using nonlinear, static analysis. Such a nonlinear model was developed for a single column using a standard analysis program (DRAIN-2DX; Prakash et al. 1993). The model parameters were determined from the bent geometry, bent reinforcement, and measured properties of the concrete, reinforcement, and fill. The objective of the analysis was to investigate whether a common analytical model would reproduce the observed behavior.

The model consisted of the following components: nonlinear beam elements, representing the column; rotational springs at the top and bottom of the column, representing the restraint provided by the crossbeam and the soil beneath the spread footing; and nonlinear translational springs, representing the resistance provided by the soil along the column length. This arrangement is shown in Fig. 10. The column was discretized into segments as shown in the figure to capture the yielding that occurs at the top and along the lower length of the column. The model was loaded with a single lateral force applied at the top of the column.

The column flexural properties were determined using a layered cross-sectional analysis based on the measured material properties. The resulting moment-curvature relationship was approximated as bilinear. Since hinging at the top of the column was concentrated in a short length, and produced large curvatures, no hardening was used at the top of the model.

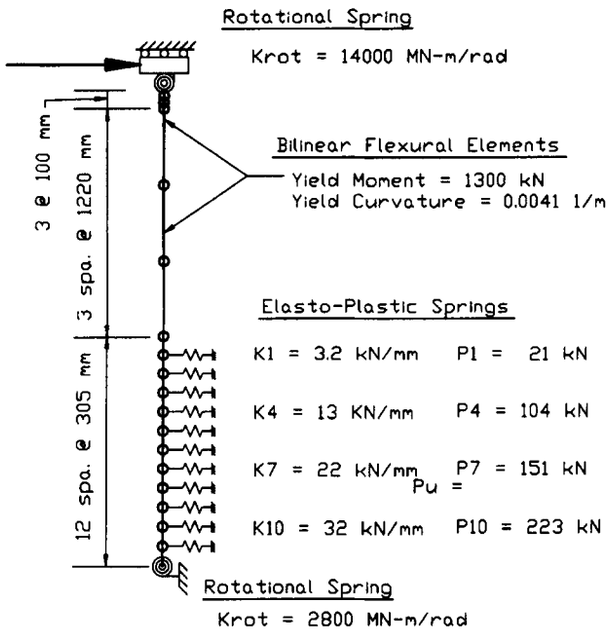


**FIG. 10. Analytical Model of Column**

The top yield moment was 1,300 kN-m, and the corresponding yield curvature was 0.0041/m. The top of the column was not permitted to yield over the first half of the plastic hinge (200 mm). Over the lower length of the column, the corresponding yield moment was 1,025 kN-m, and the hardening rate was 1.2% of the initial flexural stiffness. The yield moment and hardening rate were determined iteratively such that the final moments would be consistent with the computed moment-curvature relationship.

The nonlinear resistance of the translational soil springs were determined from the soil properties listed in Table 1 using a *p-y* curve approach described by O'Neill and Murchison (1983). According to this approach, the lateral resistance of the soil at each depth depends on the soil unit weight, the column diameter, the angle of internal friction, and the depth. The force-deformation relationship (*p-y* curve) is

$$p = p_u \tanh\left[\frac{kz}{p_u} y\right] \tag{2}$$

where $p_u$ = ultimate soil resistance; $k$ = subgrade modulus (0.047 N/mm$^3$ for $\phi = 38°$); and $z$ = soil depth. For simplicity, the force-deformation relationship computed with O'Neill and Murchison (1983) procedure was approximated with an elastoplastic relationship. Typical stiffnesses and strengths for a 305 mm length of column are shown in Fig. 10 for several depths.

The stiffness of the rotational spring at the top of the column accounted for the composite action of the crossbeam, diaphragm, and deck. The rotational stiffness at the base of the column was estimated assuming a Winkler foundation, that the footing was rigid, and that the subgrade modulus was 0.0475 N/mm$^3$.

## COMPARISON OF MEASURED AND CALCULATED RESPONSES

The lateral load-displacement relationship for a single column is shown in Fig. 11 for the analytical model and for the actual columns. The curves for the measured response represent the envelopes of all the cycles of loading applied to the bridge. Fig. 11 shows envelopes for loading cycles to the north and for loading cycles to the south.

Although the model underestimated the columns' initial

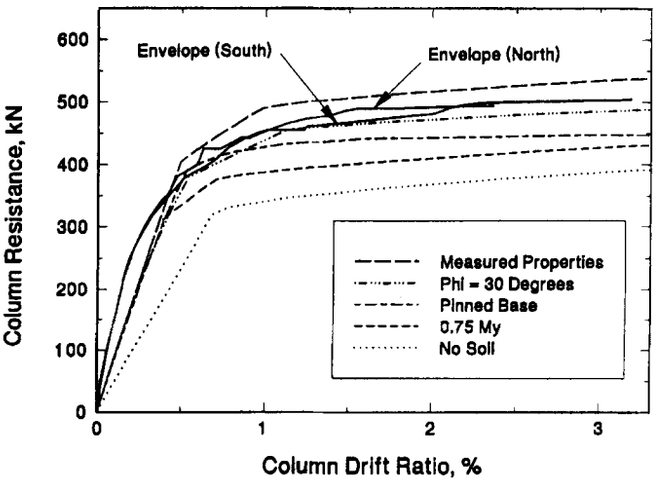


**FIG. 11. Computed and Measured Force-Displacement Responses**

stiffness, the force-displacement relationship computed with the measured material properties was similar to that measured in the field, particularly for drift ratios above 0.25%. In the model, the column first yielded at the top at a drift ratio of 0.5%. Yielding next occurred at a distance of 1.5 m above the footing at a drift ratio of 1%. Ultimately, column yielding extended from a distance of 0.6 m above the footing to 2.1 m above the footing. The maximum computed column shear was 7% larger than that measured in the field.

The model also successfully reproduced local behavior. The curvatures had been measured over a total length of 690 mm at the tops of the columns. To provide a single experimental benchmark, the curvatures measured over this length were averaged for all four columns, for both cycles at each drift level, and for loadings to the north and south. The computed curvatures were also averaged over this length. At a drift of 1%, the ratio of the analytical and the measured curvatures was 0.83. At 2% drift, the ratio was 0.93, and for 3%, it was 0.84.

In the field, the maximum crack widths had been measured in a region 1.2–2 m above the top of the footing. In comparison, the maximum plastic hinge rotations in the lower section occurred in the model between 1.5 and 1.8 m above the footing. The model also successfully reproduced the footing rotation, although the measured rotations were quite small (only three times the resolution of the instruments). The maximum rotation of the spread footing was 0.18° for the analytical model, as compared with the maximum measured rotation of approximately 0.15°.

The curvature and displacement ductility demands were estimated earlier based an assumed location of the inflection point. A second set of estimates was made using the results of the analytical model. The ductility demand was calculated from the computed plastic rotations at the top hinge, the computed inflection point location, the nominal plastic hinge length (Priestley et al. 1994), and the computed yield curvature. The curvature ductilities for 1.5 and 3% drift ratios were 9 and 21. Considering the top of the column as a cantilever with its length equal to the calculated shear span, the displacement ductilities for the top hinge were 4.5 and 10 for drift ratios of 1.5 and 3%. These results are similar to those obtained from the earlier, simpler calculations.

## SENSITIVITY OF CALCULATED RESPONSE

Additional analyses were performed to investigate the sensitivity of the calculated response to the modeling assumptions. Four parameters were varied, one at a time, from the

values used in the "measured properties" model. The results are shown in Fig. 11.

The soil internal angle of friction was reduced to 30°, a low value for typical engineered soils. This change reduced the maximum shear by 10%.

A pinned column base was simulated by removing the rotational restraint at the base of the column. This change reduced the maximum shear by 17%.

The column yield moment was reduced by 25% to take into account the difference between the nominal and actual concrete and steel properties (Table 1). The effect was to reduce the maximum shear by 20%.

Removing the soil springs along the length of the column resulted in the largest effect. For this case, the maximum shear was reduced by about 25%. At low drift ratios, the reduction was even larger. For example, the resistance provided by the "no soil" model at a drift ratio of 0.5% was only 60% of the resistance provided by the "measured properties" model at the same drift.

The implications of the parametric study were that all the resistance mechanisms, such as the soil and material overstrength, should be considered in predicting lateral response. However, the computed response was not strongly sensitive to magnitudes assigned to each component of resistance. Consequently, to estimate the seismic vulnerability of the test bridge, it would not have been necessary to perform extensive materials sampling and soil evaluation.

## CONCLUSIONS

1. Despite having minimal transverse reinforcement, short lap splices, and no top reinforcement in the footings, the two bents resisted cyclic transverse forces equal to nearly 40% of the bridge's weight at a drift ratio of 3%. The ductile response was attributed to the low shear demand and to the redistribution of rotations caused by the compacted soil that surrounded the column bases.
2. Significant spalling began at a drift ratio of approximately 1.5%. At this drift, the displacement ductility ratio was approximately 4, the curvature ductility ratio was approximately 9, and the corresponding maximum concrete compression strain was approximately 0.01.
3. Based on the measured response, it was possible to make rough estimates of the bents' seismic vulnerability. An earthquake with an effective acceleration of $0.2g$ would be expected to cause only minor flaking and spalling at the tops of the columns. Spalling would begin to occur at an effective acceleration of approximately $0.4g$. A strong earthquake with an effective acceleration of $0.6g$ would likely cause widespread spalling at the tops of the columns, but collapse would be unlikely. To extrapolate these estimates to other bridges, it would be necessary to consider the differences in shear demand, axial loads, details, and soil conditions.
4. The results of these tests should serve as benchmarks against which to evaluate existing and proposed analytical procedures. The analytical model used in this study was developed following common procedures. This model successfully reproduced the measured bent force-displacement envelope, maximum footing rotation, and the column rotations at the top of the columns. The calculated curvature distribution was consistent with the observed damage.
5. To estimate column shear demand with nonlinear analysis, it was necessary to model the effects of the soil and increases in actual material properties above their nominal values. However, the computed response was not highly sensitive to small variations in the properties of the soil and column.

## ACKNOWLEDGMENTS

The research was funded primarily by the Washington State Department of Transportation (WSDOT) and the Federal Highway Administration. H. Coffman and E. Henley served as the WSDOT technical contacts. T. O'Donovan and G. Hjartarson conducted the tests as part of their master's thesis work at the University of Washington. O'Donovan was supported by the U.S. Army, and Hjartarson was supported by the Valle Foundation at the University of Washington.

## APPENDIX. REFERENCES

*AASHTO LRFD bridge design specifications.* (1994). Am. Assn. of State Hwy. and Transp. Officials, Washington, D.C.

Eberhard, M. O., and Marsh, M. L. (1997). "Lateral-load response of reinforced concrete bridge." *J. Struct. Engrg.*, ASCE, 123(4), 451–460.

Eberhard, M. O., MacLardy, J. A., Marsh, M. L., and Hjartarson, G. (1993). "Lateral-load response of a reinforced concrete bridge." *Tech. Rep. WA-RD 305.2*, Washington State Dept. of Transp., Olympia, Wash.

O'Donovan, T. O., Eberhard, M. O., and Marsh, M. L. (1994). "Lateral-load response of two reinforced concrete piers." *Tech. Rep. WA-RD 305.3*, Washington State Dept. of Transp., Olympia, Wash.

O'Neill, M. W., and Murchison, J. M. (1983). "An evaluation of P-Y relationships in sands." *Rep. PRAC 82-41-1*, Am. Petr. Inst., Houston, Tex.

Park, R., and Paulay, T. (1975). *Reinforced concrete structures.* John Wiley & Sons, Inc., New York, N.Y.

Paulay, T., and Priestley, M. J. N. (1992). *Seismic design of reinforced concrete and masonry buildings.* John Wiley & Sons, Inc., New York, N.Y.

Prakash, V., Powell, G. H., and Campbell, S. (1993). "DRAIN-2DX base program description and user guide." *Rep. No. UCB/SEMM-93-17*, Dept. of Civ. Engrg., Univ. of California, Berkeley, Calif.

Priestley, M. J. N., Seible, F., and Chai, Y. H. (1992). "Design guidelines for assessment, retrofit, and repair of bridges for seismic performance." *Rep. No. SSRP-92-01*, Dept. of Appl. Mech. and Engrg. Sci., Univ. of California, San Diego, Calif.

Priestley, M. J. N., Seible, F., and Uang, C. M. (1994). "The Northridge earthquake of January 17, 1994: damage analysis of selected bridges." *Rep. No. SSRP-94-06*, Dept. of Appl. Mech. and Engrg. Sci., Univ. of California, San Diego, Calif.

Thewalt, C., and Stojadinovic, B. (1995). "Behavior of bridge outrigger knee-joint systems." *Earthquake Spectra*, 11(3), 477–509.